

## Observation of flux flow in superconducting $\text{YBa}_2\text{Cu}_3\text{O}_{7-\delta}$ films

H. A. Blackstead and D. B. Pulling

*Physics Department, University of Notre Dame, Notre Dame, Indiana 46556*

J. S. Horwitz and D. B. Chrisey

*Naval Research Laboratory, Washington, D.C. 20375*

(Received 1 December 1993; revised manuscript received 14 February 1994)

Measurements of field-induced changes of the  $a$ - $b$  plane surface resistance of high-quality ( $> 10^{10}$  A/m<sup>2</sup> at 77 K and  $B=0$ )  $\text{YBa}_2\text{Cu}_3\text{O}_{7-\delta}$  films at 12.92 GHz reveal flux-flow resistivity at temperatures several degrees below the superconducting onset temperature. Flux-flow resistivity is identified by its temperature dependence and dependence on the Lorentz force. The results are compared to the surface resistance theory of Coffey and Clem, which includes a model for pinning.

One of the primary reasons for the growing interest in high-frequency studies of superconductors lies in the ability of these measurements to elucidate the role of pinning in vortex dynamics. A clear understanding of pinning may contribute information essential to the successful exploitation of high-temperature materials. Microwave-frequency experiments probe the vortex response for very small amplitude vibrations, such that vortices may exhibit dissipative response (flux flow), even while pinned. This results because the vibration amplitude is estimated to be on the order of an angstrom. In contrast, dc or low-audio-frequency techniques are expected to involve the macroscopic motion of vortices, or vortex bundles. In the results to be presented, surface resistance measurements with variable angles between the rf current and the applied field will be featured, with emphasis on the response observed with  $\mathbf{J}\parallel\mathbf{B}$ . It will be demonstrated that unexpected, relatively large, field-dependent responses are observed with this configuration. The importance and relevance of the work of Lee and Stroud<sup>1</sup> will be discussed in this context. These authors have demonstrated that a network of junctions gives rise to a temperature-dependent transition width, which may be field broadened, even with  $\mathbf{J}\parallel\mathbf{B}$ . Phillips<sup>2</sup> has proposed a microscopic model for junctions, while he showed to be essential to the understanding of the high-temperature resistivity of Bi-Sr-Ca-Cu-O. Recently, Chakravarty *et al.*<sup>3</sup> have proposed that interlayer tunneling enhances the superconducting transition temperature of the layered cuprate materials. It will be suggested that the Lorentz force on vortices, arising from a  $c$ -axis tunneling current, may be responsible for the large resistive losses observed with nominal  $\mathbf{B}\parallel\mathbf{J}$  configuration. The theoretical surface resistance model due to Clem and Coffey,<sup>4-6</sup> to which the data will be compared, includes both vortex-pinning and flux-creep effects. The vortex mobility described in this theory in the limit as the frequency approaches zero includes a model for the dc resistivity. Thus, high-frequency measurements may also be expected to reflect the temperature and field dependence of the dc resistivity, as permitted by the frequency dependence. Previously,<sup>7-11</sup> it has been shown that the dc resistivity

of Y-Ba-Cu-O and Bi-Sr-Ca-Cu-O could be described in terms of flux flow and  $a$ - $b$  plane isotropic phase-slip resistivities; these dc effects<sup>12-16</sup> may be observed in microwave-frequency surface resistance measurements. The dc data discussed in the above references are never dominated by conventional flux flow; in fact, it is often unidentifiable.

Pulsed-laser-deposited thin ( $\sim 0.5$   $\mu\text{m}$ ) films of  $\text{YBa}_2\text{Cu}_3\text{O}_{7-\delta}$  prepared as described elsewhere,<sup>17</sup> were deposited on 0.010-in.-thick MgO substrates. The films were examined inductively using a multturn coil pressed against the film, to induce surface currents. Changes in the coil's inductance and the third harmonic of the driving voltage were used to determine  $T_c$  and  $J_c$ , respectively.<sup>18,19</sup> The films had a critical current density exceeding  $10^{10}$  A/m<sup>2</sup> at 77 K. X-ray diffraction indicated that the films were exclusively  $c$  axis oriented. Pole figure analysis of the (012) peak of similar films indicated a continuum of  $a$ - $b$  in-plane misorientations dominated by [100] YBCO  $\parallel$  [100] MgO and to a lesser extent [110] YBCO  $\parallel$  [110] MgO, i.e., 90° and 45° misorientations, respectively.<sup>20</sup> The microwave (12.92 GHz) spectrometer employed differs in one essential respect from conventional electron spin resonance systems: this spectrometer employs no magnetic-field modulation. Instead, this system utilizes low-drift dc amplifiers to process the point-contact microwave diode signals. Using an automatic frequency-control (AFC) circuit, the klystron signal source is frequency "locked" to the resonant frequency of the rectangular sample-bearing cavity. As a result, the system is quite insensitive to changes in the sample reactance, which tend to change the resonant frequency of the cavity. Such changes are noted only as deviations of a correction voltage as the sample is cooled through the transition region, just below the onset temperature, in zero applied field. Changes in the resonant frequency are too small to be observed in field sweeps varying to a maximum of 2 T. The rf power levels input to the cavity, which has a quality factor,  $Q \sim 1500$ , produce a rf magnetic-field amplitude  $\sim 0.1$  G at the sample surface. For these studies, the sample was mounted at the center

of the bottom which allows the static field to be rotated in the  $a$ - $b$  plane, relative to the rf current. Since the rectangular resonant cavity operates in the transverse electric TE<sub>101</sub> mode, the rf magnetic field to which the sample is exposed is uniform, parallel to the long dimension of the cavity wall, and the current density direction is well defined in the plane of the sample. The static field is also applied in the sample ( $a$ - $b$ ) plane, and can be rotated in that plane, defining the angle  $\varphi$  between the current and field directions.

Clem and Coffey (CC) have considered the problem of

surface impedance of a type-II superconductor; their analysis, which does not include junction or fluctuation effects, describes the surface impedance in terms of complex penetration depths  $\lambda_\gamma(\omega, B, T)$ , and  $\lambda_\beta(\omega, B, T)$ . Except for very close to the transition temperature  $|\lambda_\gamma| > |\lambda_\beta|$ . Because  $|\lambda_\gamma|$  for temperatures in the vicinity of  $T_c$  is of the order of micrometers (greater than typical film thicknesses), it is necessary to construct the solution appropriate to thin films. Using the CC results, and following Ramo, Whinnery, and Van Duzer,<sup>21</sup> the surface resistance of a film of thickness  $d$  is given by

$$R_s = \omega\mu_0 \left\{ \frac{\sin^2(\varphi)[\lambda_{2\gamma}\sinh(2d\lambda_{1\gamma}/|\lambda_\gamma|^2) + \lambda_{1\gamma}\sin(2d\lambda_{2\gamma}/|\lambda_\gamma|^2)]}{[\cosh(2d\lambda_{1\gamma}/|\lambda_\gamma|^2) - \cos(2d\lambda_{2\gamma}/|\lambda_\gamma|^2)]} + \frac{\cos^2(\varphi)[\lambda_{2\beta}\sinh(2d\lambda_{1\beta}/|\lambda_\beta|^2) + \lambda_{1\beta}\sin(2d\lambda_{2\beta}/|\lambda_\beta|^2)]}{[\cosh(2d\lambda_{1\beta}/|\lambda_\beta|^2) - \cos(2d\lambda_{2\beta}/|\lambda_\beta|^2)]} \right\}. \quad (1)$$

As  $T \rightarrow T_c$ ,  $\lambda_\gamma, \lambda_\beta \rightarrow (1+i)\delta_n/2$ , and for films in which  $d \ll |\lambda_\gamma|$ ,  $R_s = \rho_n/d$ , the well-known limit for a thin film. In the limit of a bulk sample ( $d \gg |\lambda_\gamma|$ ) with the applied field in the  $a$ - $b$  plane, the expression (1) for the surface resistance reduces to

$$R_s = \omega\mu_0[\lambda_{2\gamma}\sin^2(\varphi) + \lambda_{2\beta}\cos^2(\varphi)]. \quad (2)$$

Here  $\omega$  is the angular microwave frequency,  $B$  the applied field,  $T$  the temperature, and  $\varphi$  the angle between the applied field and the rf current in the  $a$ - $b$  plane. For a field in the  $a$ - $b$  plane,  $\theta = \pi/2$ , and this is the only case treated here. The several relationships are defined:

$$\lambda_\gamma^2(\omega, B, T, \varphi) = \{\lambda^2(B, T) + i/2\delta_{vc}^2(B, T, \omega)\} / \{1 - 2i\lambda^2(B, T)/\delta_{nf}^2(B, T, \omega)\}, \quad (3)$$

$$\lambda_\gamma = \lambda_{1\gamma} + i\lambda_{2\gamma}, \quad (4)$$

$$\lambda_\beta^2(\omega, B, T) = \{\lambda^2(B, T) + i/2\delta_{vc}^2(B, T, \omega)\cos^2(\theta)\} / \{1 - 2i\lambda^2(B, T)/\delta_{nf}^2(B, T, \omega)\}, \quad (5)$$

$$\lambda_\beta = \lambda_{1\beta} + i\lambda_{2\beta}, \quad (6)$$

$$\delta_{nf}^2(\omega, B, T) = (2\rho_n/\mu_0\omega) / \{1 - [1 - (T/T_c)^4](1 - B/\{H_{c20}[1 - (T/T_c)^2]/[1 + (T/T_c)^2]\})\}, \quad (7)$$

$$\lambda(B, T) = \lambda(0) / \{[1 - (T/T_c)^4](1 - B/\{H_{c20}[1 - (T/T_c)^2]/[1 + (T/T_c)^2]\})\}^{1/2}, \quad (8)$$

$$\mu(\omega, T) = 1/\eta[1 + (-i\omega\eta/\alpha\kappa_{\rho 0} + 1/\{I_0^2[U(1 - T/T_c)^{3/2}/B] - 1\})^{-1}]^{-1}, \quad (9)$$

$$\rho_v(\omega) = B\phi_0\mu(\omega, T), \quad (10)$$

$$\eta = \phi_0 H_{c2}/\rho_n, \quad (11)$$

$$\delta_{vc}^2 = 2\rho_v(\omega)/\mu_0\omega. \quad (12)$$

The viscosity is  $\eta$ ,  $\rho_n$  is the normal resistivity,  $\rho_v$  is the vortex resistivity,  $\mu_v$  is the vortex mobility,  $\lambda$  is the penetration depth,  $\phi_0$  is the flux quantum, and  $H_{c2}$  is the upper critical field. Here  $\kappa_{\rho 0}$  is the force constant of the pinning potential,  $\alpha = I_1(\nu)/I_0(\nu)$  where  $I_p$  is a modified Bessel function with  $\nu = U(1 - T/T_c)^{3/2}/B$ , and  $U$  is a constant. The microwave system measures field-induced changes in  $R_s$  which are given by

$$\Delta R_s(B, T, \varphi) = R_s(B, T, \varphi) - R_s(B=0, T, \varphi). \quad (13)$$

Angular-dependent changes in the surface resistance at constant  $B$  are given by

$$\Delta R_s(\varphi) = R_s(B = \text{const}, T, \varphi) - R_s(B = \text{const}, T, \varphi=0). \quad (14)$$

Fitting the temperature-dependent data to Eq. (13) gave  $H_{c20} = 130\Gamma$  T (this is appropriate for fields applied in the  $a$ - $b$  plane), with the mass anisotropy ratio  $\Gamma = 5$  [ $\Gamma = (m_c/m_{a-b})^{1/2}$ ] and provides  $dH_{c2}/dt = -1.47$  T/K, in reasonable agreement with other experiments.<sup>22</sup> Several parameters determined in evaluating these functions include  $\lambda(0) = 4000$  Å,  $U > 1$  μeV, and  $\kappa_{\rho 0} < 1 \times 10^{-8}$  N/m<sup>2</sup>. The results are very insensitive to  $\kappa_{\rho 0}$  and  $U$ , provided that  $\kappa_{\rho 0}$  is small and  $U$  is finite. It is useful to note that, in the limit that  $\kappa_{\rho 0} \rightarrow 0$ ,

$\mu=1/\eta$  and  $\rho_v(\omega)=\rho_n B/H_{c2}$ . The other interesting limit, in which  $\kappa_{\rho 0} \rightarrow \infty$  describes perfect pinning. We take  $\rho_n(T)=(0.8T/T_c+0.2)0.5\mu\Omega\text{m}$ , a form similar to the one employed by CC, which provides for a residual value at  $T=0$ , and gives a good fit to the data. The resistivity at  $T_c$  is typical of these films; since the spectrometer is not calibrated for absolute surface resistance determinations, the scale of the several figures is specified as arbitrary. The film thickness was  $0.6\mu\text{m}$ , and  $T_c=89.4\text{K}$ . The transition temperature was determined by both  $J_c$  measurements and the microwave data. Because the CC model does not include a description of the finite dc  $B=0$  transition width,<sup>23,24</sup> the calculations used a different  $T_c=88.5\text{K}$  in order to place the peak temperature-dependent response at approximately the same temperature as the experimental result. The value determined for  $\lambda(0)$  is in significant disagreement with published results; with a more appropriate smaller value ( $1200\text{--}1400\text{\AA}$ ), the data are not well described by this model. The size of  $\kappa_{\rho 0}$  and  $U$  describes an effective response with no significant flux creep.

The field-dependent reactive response leads to changes in the resonant frequency of the cavity; the automatic frequency-control circuit employed in the spectrometer nulls out the sample-induced frequency changes and so the system responds only to changes in the surface resistance. The power dissipation in the sample mounted on the wall of the microwave resonant cavity is given by the surface integral,  $P=\frac{1}{2}\int|H_{\text{rf}}|^2R_s ds$ , and the detected signals are proportional to this quantity. As a consequence of the form of (1), and the feature that  $|\lambda_\beta|$  is small compared to  $|\lambda_\gamma|$ , we may anticipate that, for temperatures approaching the transition temperature, flux flow and flux creep with  $B$  in the sample plane will vary as  $\sin^2(\varphi)$ . During the experiment, the input power to the cavity is maintained at a constant level; as a result, the rf field intensity is essentially constant, and field-induced changes in the dissipation are proportional to changes in the surface resistance. The induced current densities associated with the rf penetration depth are very large, and with the use of a microwave cavity may vary with power level from approximately<sup>25</sup>  $10^7$  to  $10^9\text{A/m}^2$ . These high current densities are typically 2–4 orders of magnitude larger than current densities employed in conventional dc or low-frequency techniques which are employed to characterize  $T_c$  and the width of the transition. With  $B=0$ , the flux-flow contribution vanishes, but a frequency-dependent residual surface resistance, typically on the order of  $m\Omega$  at low temperatures,<sup>17</sup> is observed even in high-quality (high- $J_c$ ) materials.

In the following, variation of the surface resistance with the field intensity, the field orientation, and the temperature will be explored and compared to the results of the Coffey-Clem model. Figure 1 illustrates field scans with  $B$  perpendicular to the rf current in the plane of the film as a function of temperature and applied field. The peak in the dissipation as a function of temperature, at any fixed field, is a consequence of the rapid drop of the resistivity just below the transition temperature, and the field-broadened resistivity. Figure 2 illustrates the dissi-

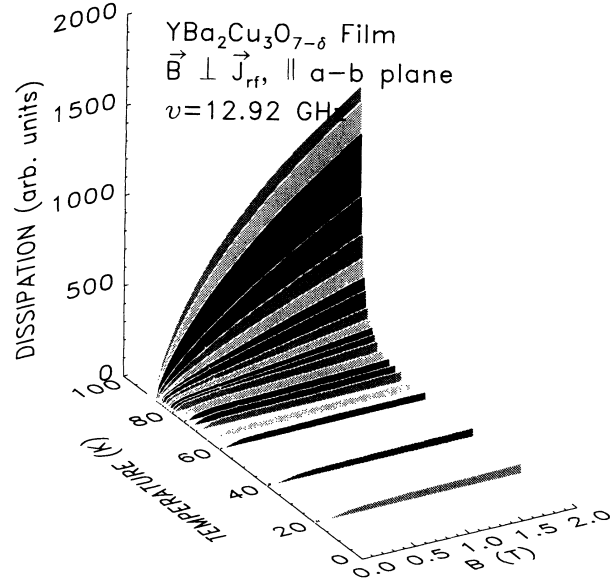


FIG. 1. Field scans with  $B$  in the film plane, perpendicular to the rf current (also in the plane of the sample), as a function of temperature. The changes in dissipation are proportional to field-induced changes in the surface resistance. The peak in the response (at any fixed field) arises as a consequence of the rapid decrease in the temperature-dependent resistivity through the transition with  $B=0$ , and the field-induced increase of the surface resistance.

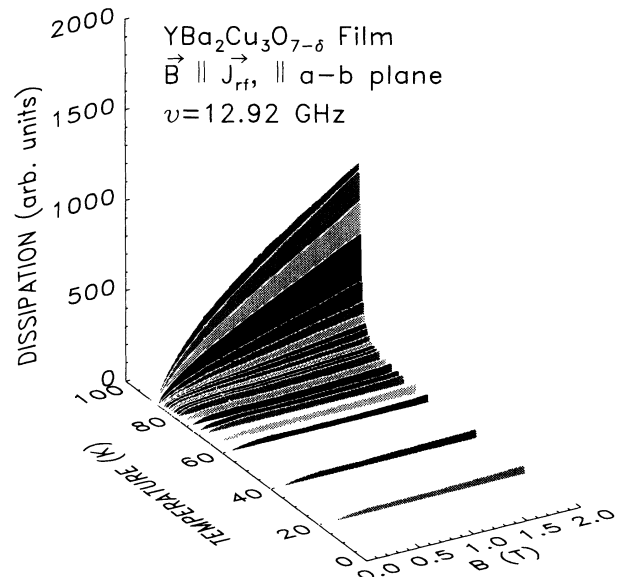


FIG. 2. Field scans with  $B$  in the film plane, parallel to the rf current (also in the plane of the sample), as a function of temperature. The changes in dissipation are proportional to field-induced changes in the surface resistance. Since the instrument does not have an absolute calibration, the scale has arbitrary units.

pation observed with  $\mathbf{B} \parallel \mathbf{J}$ , also in the  $a$ - $b$  plane. In Fig. 3, a profile of the data for  $B$  perpendicular and parallel to the rf current, with the field in the plane, is illustrated at a fixed field of 1.5 T. The resulting overall fit to Eqs. (1) and (13) is quite satisfactory. With a fixed field of 1.0 T, rotations ( $\varphi$ ) in the sample plane were obtained (see Fig. 4). These rotations directly reveal the conventional Lorentz-force-dependent variation of the surface resistance, which in this model arises from flux flow and flux creep. However, the parameters of the fit to the temperature-dependent data effectively render the response as due to flux flow. In Fig. 5, data sets at 88.25, 88.0, 87.5, 87, and 86 K, are plotted along with the model computations. The data were scaled to match the modeled results of Fig. 4; the model quite accurately reproduces the distinctive qualitative feature of the response, the approximate  $\sin^2(\varphi)$  dependence, but fails to describe the angular-independent field and temperature-dependent “background.” The flux-flow amplitude illustrated in this sequence is the largest (as large as  $\sim 60\%$  of the total) reported for a high-temperature superconductor (HTSC). For comparison, see Refs. 11–16. It has been our experience that the Lorentz-force-driven amplitude *rarely* exceeds 20% of the signal. This is the largest flux-flow (Lorentz-force-dependent) amplitude ever reported to our knowledge for a HTSC material which resulted from a surface resistance measurement, and is the principal experimental finding of this paper.

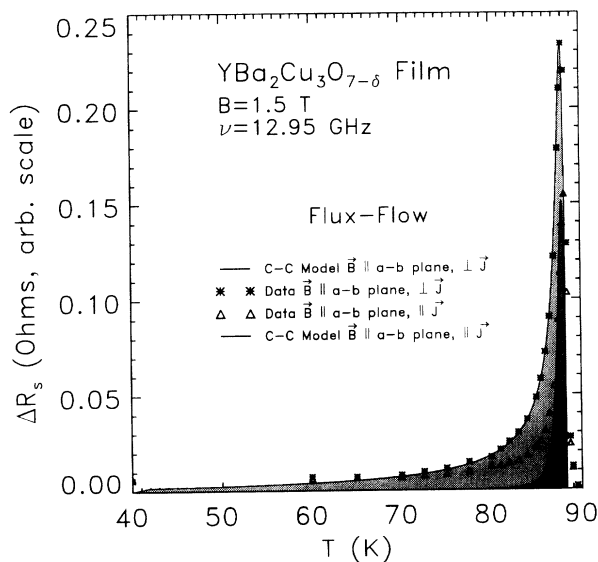


FIG. 3. Superconducting dissipation data as determined by  $\Delta R_s$  at a fixed field of 1.5 T and 12.95 GHz as function of temperature for the applied field parallel to the  $a$ - $b$  plane and parallel and perpendicular to the rf current. The gray-scale insets show the modeled changes in surface resistance as given by (1). The data were multiplied by one constant, selected to match the model computation at the peak of dissipation with  $\mathbf{B}$  perpendicular to  $\mathbf{J}$ . The computed peak with  $\mathbf{B}$  parallel to  $\mathbf{J}$  is in agreement with the data, but the model results fall off with reduced temperature more rapidly than do the data.

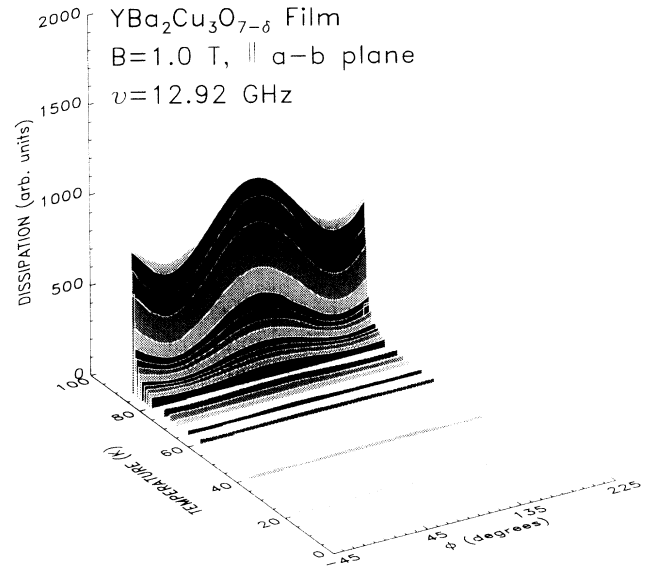


FIG. 4. Rotary scans in the sample ( $a$ - $b$ ) plane at  $B=1.0$  T. At temperatures near  $T_c$ , atypical flux-flow characteristics are evident; the Lorentz-force-dependent response is the largest ( $\sim 60\%$ ) ever reported to our knowledge; angular-dependent changes of 10–15% are typical, even in high-quality material. At lower temperatures, the dissipation is greatly reduced in amplitude, but small angular-dependent changes are noted. There is no evidence for twin-boundary pinning effects.

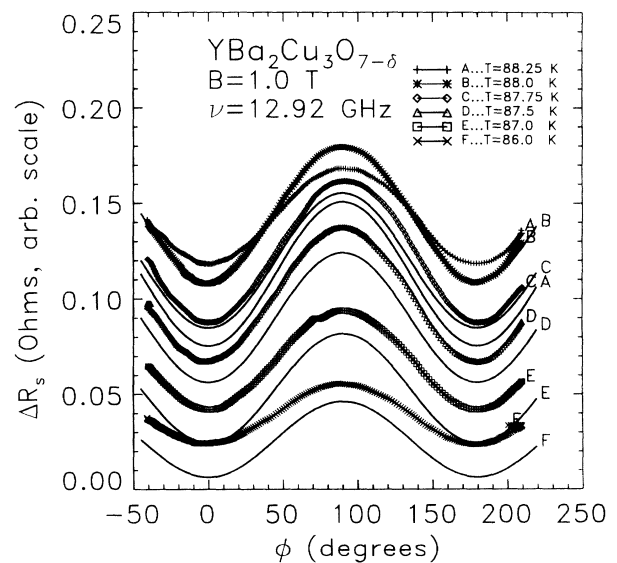


FIG. 5. Six of the data sets of Fig. 4, at 88.25, 88, 87.75, 87.5, 87, and 86 K, are plotted along with the model computations. The data may be represented as a response proportional to  $\sin^2(\varphi)$ , superimposed on a field- and temperature-dependent axially symmetric background. The data were scaled by a constant factor, to match the model computation at the peak of the response for  $B=1$  T. The amplitude of the data falls, as compared to the model, as the temperature is reduced. This is a consequence of the larger experimental “background” surface resistance with  $\mathbf{B} \parallel \mathbf{J}$ .

These surface resistance data are very similar to the low-frequency ( $\sim$ dc) data of Kwok *et al.*,<sup>26</sup> which also illustrate a  $\sin^2(\varphi)$ -dependent resistivity superimposed on a field- and temperature-dependent "background." It is important to note that dc resistivity measurements on high-quality films in the *a-b* plane reveal isotropy.<sup>27</sup> Only on very high-quality samples, such as those measured by Kwok *et al.*, has flux flow (and possibly flux creep) been observed at low current densities and low (audio) frequencies. At microwave frequencies, such observations are routine; the microwave-frequency measurements tend to render the pinning ineffective. However, we have observed twin-boundary pinning<sup>12</sup> in surface resistance measurements on crystalline Y-Ba-Cu-O over a range of temperatures, varying by approximately 65 K. We make such observations routinely in heavily twinned specimens.<sup>14</sup> It is an inevitable conclusion that the microwave-frequency measurements *are* sensitive to pinning. The Kwok *et al.* data also reveal twin-boundary pinning. Pinning severely limits the ability of dc resistivity measurements to detect Lorentz-force-dependent (flux-flow and flux-creep) effects. At microwave frequencies, the fluxon vibration amplitude is on the order of 1 Å,<sup>28</sup> while dc flux flow and flux creep engender macroscopic flux displacements. The conventional flux-flow contribution, identified by Lorentz-force-dependent variation and characteristic temperature dependence, is seen generally to be a small contribution to the resistivity which vanishes as the temperature approaches  $T_c$ . However, a few degrees below the transition temperature, these films exhibit unusually large (as a fraction of the total surface resistance) flux flow. Jiang *et al.*<sup>29</sup> demonstrated that films similar to the ones studied here were able to support ultrahigh critical current densities, as large as  $1.3 \times 10^{13}$  A/m<sup>2</sup>.

Lee and Stroud<sup>2</sup> have demonstrated that a network of junctions gives rise to a transition width, which may be field broadened, even with  $J_{\parallel}B$ . Phillips<sup>2</sup> has proposed a

microscopic model for junctions, which he showed to be essential to the understanding of the high-temperature resistivity of Bi-Sr-Ca-Cu-O. Recently, Chakravarty *et al.*<sup>3</sup> have proposed that interlayer tunneling enhances the superconducting transition temperature of the layered cuprate materials. The existence of junctions in HTSC materials was confirmed by Kleiner *et al.*,<sup>30</sup> in experiments on crystalline Bi-Sr-Ca-Cu-O; the ac Josephson effect was observed, and the microwave radiation emitted from the sample, excited by a dc current, was characteristic of a network of junctions. These findings suggest a number of important results: Since junctions interior to an otherwise homogeneous superconductor would be shorted out by surrounding material, to be expressed, the junctions are likely to be part of a percolative network (a stack of series junctions along the *c* axis would not constitute a network). In order to produce a network, the materials must be highly faulted, or at least must contain regions of reduced order parameter. Such regions might give rise to a larger effective penetration depth, as suggested by the fit. If such junctions are formed as a consequence of planar imperfections, it will be natural to conclude that the nominal *a-b* plane transport currents will have a *c*-axis component. The higher quality the material, the smaller such currents will be. However, these currents are always perpendicular to a field applied in the *a-b* plane. As a result, these currents are expected to be a fraction of the total current, and forces on vortices will arise. The data presented may imply that roughly  $\frac{1}{2}$  of the current in these thin films is distributed in meandering paths.

H.A.B. and D.B.P. gratefully acknowledge support from the Midwest Superconducting Consortium through U.S. Department of Energy Grant No. DE-FG02-90ER45427. H.A.B. thanks J. C. Phillips (AT&T), H. Newman (NRL), M. Coffey (NIST), and J. R. Clem (Iowa State) for very helpful discussions.

<sup>1</sup>K. H. Lee and D. Stroud, Phys. Rev. B **46**, 5699 (1992).

<sup>2</sup>J. C. Phillips, Phys. Rev. B **46**, 8542 (1992).

<sup>3</sup>S. Chakravarty, A. Sudbo, P. W. Anderson, and S. Strong, Science **261**, 337 (1993).

<sup>4</sup>J. R. Clem and M. W. Coffey, Phys. Rev. Lett. **67**, 386 (1992).

<sup>5</sup>J. R. Clem and M. W. Coffey, Physica C **185-189**, 1915 (1991).

<sup>6</sup>M. W. Coffey and J. W. Clem, Phys. Rev. B **45**, 10 527 (1992).

<sup>7</sup>H. A. Blackstead, Phys. Rev. B **47**, 11 411 (1993).

<sup>8</sup>H. A. Blackstead, Solid State Commun. **87**, 35 (1993).

<sup>9</sup>H. A. Blackstead, Physica C **209**, 437 (1993).

<sup>10</sup>H. A. Blackstead, D. G. Keiffer, M. D. Lan, and J. Z. Liu, Superlatt. Microstruct. **13**, 279 (1993).

<sup>11</sup>H. A. Blackstead, J. Supercond. **5**, 67 (1992).

<sup>12</sup>H. A. Blackstead, D. B. Pulling, and P. J. McGinn, Physica C **175**, 534 (1991).

<sup>13</sup>H. A. Blackstead, D. B. Pulling, P. J. McGinn, and W. H. Chen, J. Supercond. **4**, 263 (1991).

<sup>14</sup>H. A. Blackstead, D. B. Pulling, and C. A. Clough, Phys. Rev. B **47**, 8978 (1993).

<sup>15</sup>H. A. Blackstead, D. B. Pulling, P. J. McGinn, and J. Z. Liu,

Physica C **174**, 394 (1991).

<sup>16</sup>H. A. Blackstead, D. B. Pulling, D. G. Keiffer, M. Sankararaman, and H. Sato, Phys. Lett. A **170**, 130 (1992).

<sup>17</sup>D. B. Chrisey, J. S. Horwitz, H. S. Newman, M. E. Reeves, B. D. Weaver, K. S. Grabowski, and G. P. Summers, J. Supercond. **4**, 57 (1991).

<sup>18</sup>J. M. Claassen, IEEE Trans. Magn. **25**, 2233 (1989).

<sup>19</sup>J. M. Claassen, M. E., Reeves, and R. J. Soulen, Rev. Sci. Instrum. **62**, 996 (1991).

<sup>20</sup>K. S. Grabowski (private communication).

<sup>21</sup>S. Ramo, J. R. Whinnery, and T. Van Duzer, *Fields and Waves in Communication Electronics* (Wiley, New York, 1965), p. 301.

<sup>22</sup>U. Welp, W. K. Kwok, G. W. Crabtree, K. G. Vandervoort, and J. Z. Liu, Phys. Rev. B **40**, 5263 (1989).

<sup>23</sup>D. A. Bonn, R. Liang, T. M. Riseman, D. J. Baar, D. C. Morgan, K. Zhang, P. Dosanjh, T. L. Duty, A. McFarlane, G. D. Morris, J. H. Brewer, W. N. Hardy, C. Kallin, and A. J. Berlinsky, Phys. Rev. A **47**, 11 314 (1993). These authors showed that the dc transition width could be measured with consider-

- able accuracy using microwave surface resistance measurements and the classical expression for the surface resistance  $R_s = \rho/\delta$ , where  $\rho$  is the dc resistivity and  $\delta$  is the conventional rf skin depth.
- <sup>24</sup>Evaluating  $\mu$  in the limit as  $\omega/\kappa_{\rho 0} \rightarrow 0$  yields a dc resistivity model which provides for a zero transition width for  $B=0$ .
- <sup>25</sup>J. D. Jackson, *Classical Electrodynamics* (Wiley, New York, 1962), p. 240. The current density in the cavity or sample can be estimated using the resistivity of copper or the normal-state resistivity of the sample at the transition temperature and the rf field amplitude.
- <sup>26</sup>W. K. Kwok, U. Welp, G. W. Crabtree, K. G. Vandervoort, R. Hulscher, and J. Z. Liu, *Phys. Rev. Lett.* **64**, 966 (1990).
- <sup>27</sup>Y. Iye, S. Nakamura, T. Tamegai, T. Terashima, K. Yamamoto, and Y. Bando, *Physica C* **166**, 62 (1990).
- <sup>28</sup>W. J. Tomasch, H. A. Blackstead, S. T. Ruggiero, P. J. McGinn, John R. Clem, K. Shen, J. W. Weber, and D. Boyne, *Phys. Rev. B* **37**, 9864 (1988).
- <sup>29</sup>H. Jiang, Y. Huang, H. How, S. Zhang, C. Vittoria, A. Widom, D. B. Chrisey, J. S. Horwitz, and R. Lee, *Phys. Rev. Lett.* **66**, 1785 (1992).
- <sup>30</sup>R. Kleiner, F. Steinmeyer, G. Kunkel, and P. Muller, *Phys. Rev. Lett.* **68**, 2394 (1992).

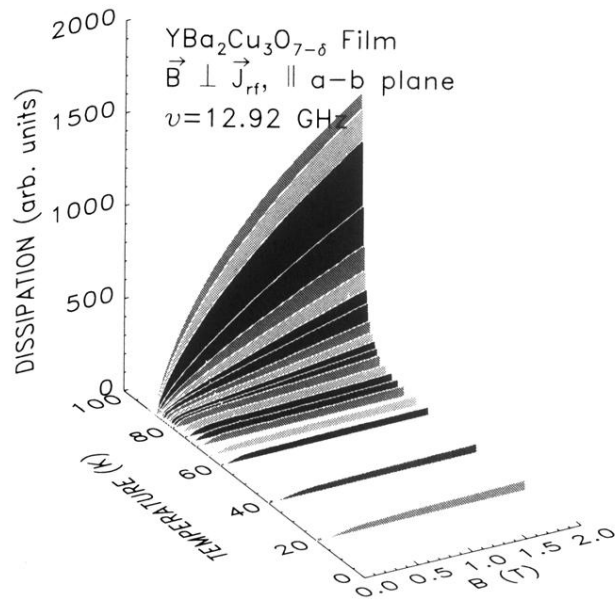


FIG. 1. Field scans with  $B$  in the film plane, perpendicular to the rf current (also in the plane of the sample), as a function of temperature. The changes in dissipation are proportional to field-induced changes in the surface resistance. The peak in the response (at any fixed field) arises as a consequence of the rapid decrease in the temperature-dependent resistivity through the transition with  $B=0$ , and the field-induced increase of the surface resistance.

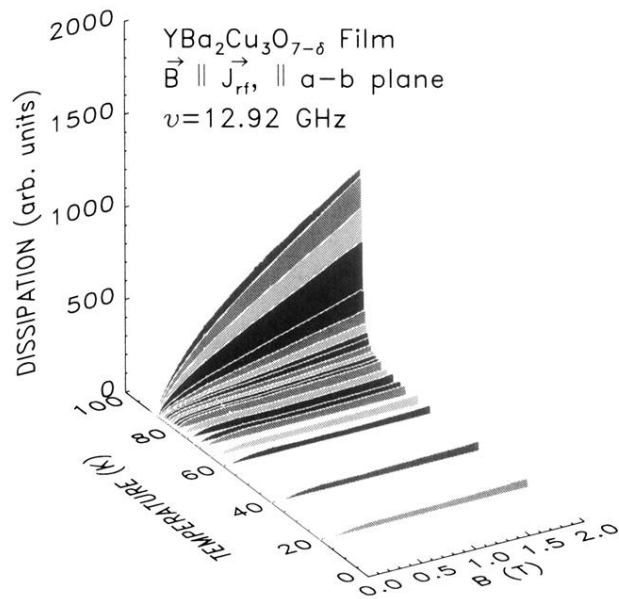


FIG. 2. Field scans with  $B$  in the film plane, parallel to the rf current (also in the plane of the sample), as a function of temperature. The changes in dissipation are proportional to field-induced changes in the surface resistance. Since the instrument does not have an absolute calibration, the scale has arbitrary units.



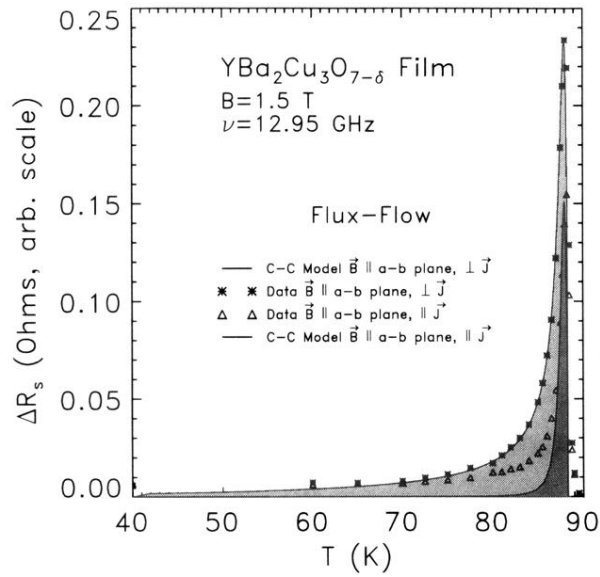


FIG. 3. Superconducting dissipation data as determined by  $\Delta R_s$  at a fixed field of 1.5 T and 12.95 GHz as function of temperature for the applied field parallel to the  $a$ - $b$  plane and parallel and perpendicular to the rf current. The gray-scale insets show the modeled changes in surface resistance as given by (1). The data were multiplied by one constant, selected to match the model computation at the peak of dissipation with  $\mathbf{B}$  perpendicular to  $\mathbf{J}$ . The computed peak with  $\mathbf{B}$  parallel to  $\mathbf{J}$  is in agreement with the data, but the model results fall off with reduced temperature more rapidly than do the data.

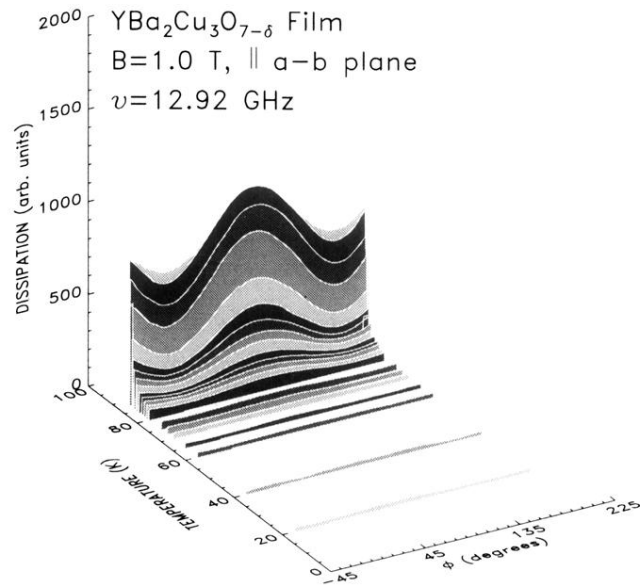


FIG. 4. Rotary scans in the sample ( $a$ - $b$ ) plane at  $B=1.0$  T. At temperatures near  $T_c$ , atypical flux-flow characteristics are evident; the Lorentz-force-dependent response is the largest ( $\sim 60\%$ ) ever reported to our knowledge; angular-dependent changes of 10–15% are typical, even in high-quality material. At lower temperatures, the dissipation is greatly reduced in amplitude, but small angular-dependent changes are noted. There is no evidence for twin-boundary pinning effects.